European Journal of Medicinal Chemistry 123 (2016) 905–915

Contents lists available at ScienceDirect

European Journal of Medicinal Chemistry

journal homepage: http://www.elsevier.com/locate/ejmech

Research paper

Studies on the inhibition of sphingosine-1-phosphate lyase by stabilized reaction intermediates and stereodefined azido phosphates

Pol Sanllehí [a, c], José-Luís Abad [a], Jordi Bujons [b], Josefina Casas [a, **], Antonio Delgado [a, c, *]

[a] Spanish National Research Council (CSIC), Institute of Advanced Chemistry of Catalonia (IQAC-CSIC), Research Unit on Bioactive Molecules (RUBAM), Department of Biomedicinal Chemistry, Jordi Girona 18-26, 08034, Barcelona, Spain
[b] Spanish National Research Council (CSIC), Institute of Advanced Chemistry of Catalonia (IQAC-CSIC), Department of Biological Chemistry and Molecular Modelling, Jordi Girona 18-26, 08034, Barcelona, Spain
[c] University of Barcelona (UB), Faculty of Pharmacy, Department of Pharmacology, Toxicology and Medicinal Chemistry, Unit of Pharmaceutical Chemistry (Associated Unit to CSIC), Avda. Joan XXIII s/n, 08028, Barcelona, Spain

ARTICLE INFO

Article history:
Received 6 July 2016
Received in revised form
4 August 2016
Accepted 5 August 2016
Available online 6 August 2016

Keywords:
Sphingolipids
Enzyme inhibitor
Sphingosine lyase
Synthesis
Stereocontrolled

ABSTRACT

Two kinds of inhibitors of the PLP-dependent enzyme sphingosine-1-phosphate lyase have been designed and tested on the bacterial (StS1PL) and the human (hS1PL) enzymes. Amino phosphates **1**, **12**, and **32**, mimicking the intermediate aldimines of the catalytic process, were weak inhibitors on both enzyme sources. On the other hand, a series of stereodefined azido phosphates, resulting from the replacement of the amino group of the natural substrates with an azido group, afforded competitive inhibitors in the low micromolar range on both enzyme sources. This similar behavior represents an experimental evidence of the reported structural similarities for both enzymes at their active site level. Interestingly, the *anti*-isomers of the non-natural enantiomeric series where the most potent inhibitors on hS1PL.

1. Introduction

Phosphorylated sphingolipids are an important group of sphingoid metabolites that present a terminal phosphate group. Among them, sphingosine-1-phosphate (S1P) is a well-recognized signaling molecule that regulates cell differentiation, survival, inflammation, angiogenesis, calcium homeostasis and immunity, among other functions [1]. Recent findings have associated high S1P levels with neuroprotective effects that counteract many noxious processes that follow CNS injury [2,3] (apoptotic cell death, lipid hydrolysis, oxidative stress and tissue damage), while supporting growth and trophic factor activities. In general, the roles of phosphorylated sphingolipids are opposed to those of ceramides (Cer), which are potent inducers of cell cycle arrest and apoptosis [4]. Thus, the control of the S1P/Cer balance might be exploitable for the discovery of potential neuro-restorative therapies with applications in traumatic brain injury, spinal cord injury, and stroke. These tissue protective properties make S1P a suitable cellular survival signaling agent, in contraposition to Cer, which is a well-recognized mediator of cellular stress responses. In addition to the intracellular functions, paracrine functions of S1P through its binding to specific lipid G-protein coupled $S1P_{1-5}$ receptors are also known. In this way, S1P becomes essential for vascular development and endothelial integrity, control of cardiac rhythm, and immunity responses [5–10].

Sphingosine-1-phosphate lyase (S1PL) is a pyridoxal 5′-phosphate (PLP) dependent enzyme, localized in the endoplasmic reticulum (ER), that catalyzes the irreversible degradation of S1P into ethanolamine phosphate (EAP) and *trans*-2-hexadecenal (Scheme 1) [11]. According to the proposed mechanism of cleavage [11], the incoming S1P replaces the catalytic Lys in internal aldimine **A** (step 1, Scheme 1) to form the external aldimine **B**. Retro-aldol cleavage takes place at the C3–OH group of S1P (step 2) to release the corresponding aldehyde. Reprotonation of the transient quinonoid intermediate **C** (step 3) leads to external aldimine **D**, from which EAP is released after hydrolysis (step 4) and the internal aldimine **A** is formed again for a second enzyme turnover. An

* Corresponding author. Spanish National Research Council (CSIC), Institute of Advanced Chemistry of Catalonia (IQAC-CSIC), Research Unit on Bioactive Molecules (RUBAM), Department of Biomedicinal Chemistry, Jordi Girona 18-26, 08034, Barcelona, Spain.
** Corresponding author.
E-mail address: delgado@rubam.net (A. Delgado).

http://dx.doi.org/10.1016/j.ejmech.2016.08.008
0223-5234/

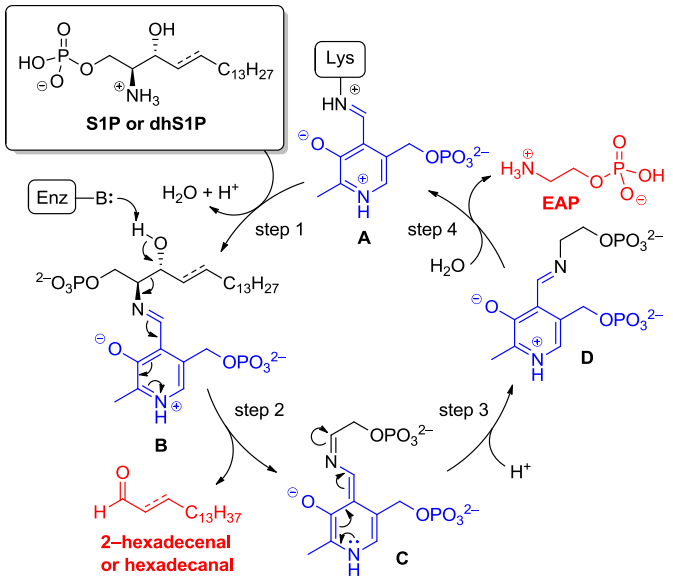

Scheme 1. Catalytic cycle of sphingosine-1-phosphate lyase (S1PL). 1) S1P or dhS1P replaces Lys from **A** to form the external aldimine **B**; 2) Retro-aldol cleavage with generation of 2-hexadecenal or hexadecanal and the quinonoid intermediate **C**; 3) Formation of the aldimine system **D** by protonation of **C**; 4) Hydrolysis of **D** with release of EAP and final restoration of **A**.

identical mechanism is accepted for the alternative S1PL substrate 4,5-dihydro-S1P (dhS1P), giving rise to EAP and hexadecanal as reaction products. The degradation of S1P by S1PL has been considered as the "exit gate" of sphingolipid metabolism and the natural connection with phospholipid metabolism through the conversion of EAP into phosphatidylethanolamine, another signaling molecule in lipid metabolism [12]. In combination with S1P phosphatase and sphingosine kinases (SK) [13], the levels of intracellular S1P can be efficiently regulated.

So far, the repertoire of available S1PL inhibitors structurally related to the enzyme substrate is scarce. In this context, 1-deoxysphinganine 1-phosphonate [14] and the 2-vinyl dihydrosphingosine 1-phosphate (2-vinyl dhS1P) (Fig. 1) are the only ones reported in the literature [15]. The structurally related **FTY720**, a well-known S1P receptor agonist after the enantioselective phosphorylation to the (*S*) isomer, has also been reported as a modest S1PL inhibitor *in vitro* [16,17]. On the other hand, the PLP antagonist 4-deoxypyridoxine (DOP) has been described as a functional S1PL inhibitor *in vivo* [18–20], as well as THI and related analogs [20,21], whose mechanism of action is controversial [22–24]. Finally, some heterocyclic compounds resulting from massive HTS programs have been discovered as potent and selective S1PL inhibitors [18–20,25], some of them with IC_{50} values in the nM range [26,27].

As a result of our interest in the development of sphingolipid modulators by targeting S1P metabolism [28], we undertook the design of new S1PL inhibitors based on S1PL mechanistic considerations. Thus, compounds **12** and **32** (Fig. 2) were designed as non-reactive analogs of the intermediate aldimine **B** (Scheme 1), whereas compound **1** (Fig. 2) can be regarded as a non-hydrolyzable analog of the putative intermediate **D** (Scheme 1). Interestingly, dephosphorylated **32** had been reported in the literature as a potential S1PL inhibitor. However, its lack of activity in cells was attributed to an inadequate phosphorylation *in vivo* [20].

As PLP analogs, compounds **1**, **12**, and **32** were expected to displace the cofactor in the enzyme active site. In a second approach, a series of configurationally defined azide analogs of both enzyme substrates (S1P and dhS1P) were designed as non-reactive, potential S1PL competitive inhibitors (compounds **89**, **98**, **103**, and **114**, Fig. 2). Since the C2-amino group in S1P is replaced by an azido group, formation of the external aldimine **B** is expected to be precluded at the enzyme active site. Apart from the inherent lack of reactivity towards imine formation and its remarkable stability *in cellulo* [29], the azido group has also been used as a "pseudohalide" in drug design [30]. In our case, the replacement of the amino group present in S1P with an azido group is expected to cause a dramatic effect in the electronic properties and on the interactions with the enzyme active site, without disturbing the overall shape of the molecule. Moreover, to gain insight into the enzyme stereoselectivity towards this type of analogs, all the configurations around the C2 and C3 carbon atoms have been considered (ie. compounds ***ent*-89**, ***ent*-98**, ***ent*-103** and ***ent*-114**).

2. Results and discussion

2.1. Synthesis

Compounds **1**, **12** and **32** were obtained as outlined in Scheme 2 by reductive amination of PLP with either *O*-phosphorylethanolamine, dhS1P or S1P, respectively. Following an adaptation of reported protocols [31,32], the corresponding dipotassium salts were generated *in situ* with KO*t*-Bu in order to ensure their total solubility. After the consumption of the starting amine was evidenced by ^{1}H NMR, reduction of the corresponding imines with $NaBH_4$ afforded the desired diphosphates in acceptable overall yields, together with pyridoxine-5′-phosphate, which was also included in our S1PL inhibition assays due to its high structural similarity with PLP and DOP. On the other hand, crude diphosphates **12** and **32** presented a very low solubility in different organic solvents and in aqueous mixtures. Nevertheless, preparation of the corresponding triethylammonium salts afforded highly water-soluble species, which could be properly characterized in terms of chemical identity and biological activity.

The synthesis of the differently configured azidophosphates was carried out from the corresponding stereodefined sphingosines, whose synthesis from D- or L-Garner's aldehyde is depicted in Scheme 3. For the 2*S* series, the *anti*-adducts resulted from the diastereoselective addition of vinylmagnesium bromide to the starting aldehyde, following a well-established reported protocol in which the *anti*-configuration of the amino diol moiety was secured by chemical correlation with a stereodefined reference compound [33]. Cross-metathesis of **23** with 1-pentadecene, in the presence of Grubbs catalyst (second generation) [34,35], followed by isopropylidene removal afforded the key sphingoid intermediate **25**, whose configuration was in agreement with the optical rotation data reported for this compound in the literature [36]. On the other

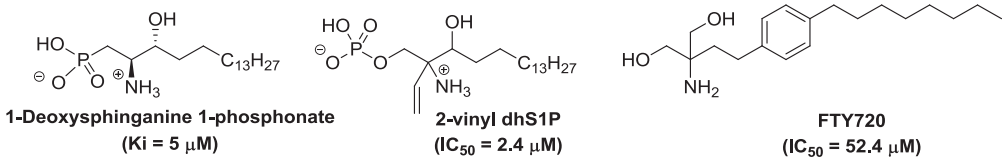

Fig. 1. Reported S1PL inhibitors structurally related with the enzyme substrate.

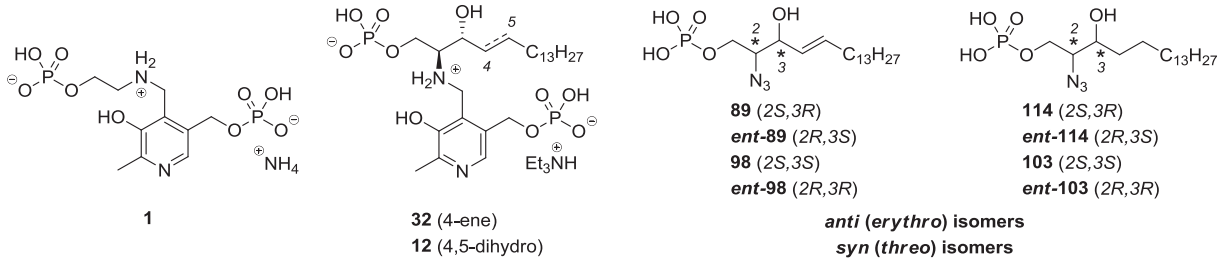

Fig. 2. Non-reactive S1PL reaction intermediates and substrates described in this work.

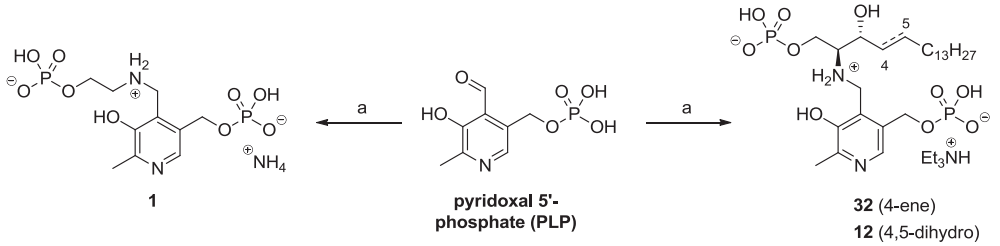

Scheme 2. Synthesis of PLP-derivatives. Reagents and conditions: (a) (i) selected amine (*O*- Phosphorylethanolamine for **1**, S1P for **32** and dhS1P for **12**), *K*Ot-Bu, MeOH, reflux (ii) $NaBH_4$, MeOH, 0 °C to rt, 79% for **1**, 74% for **32**, 71% for **12**.

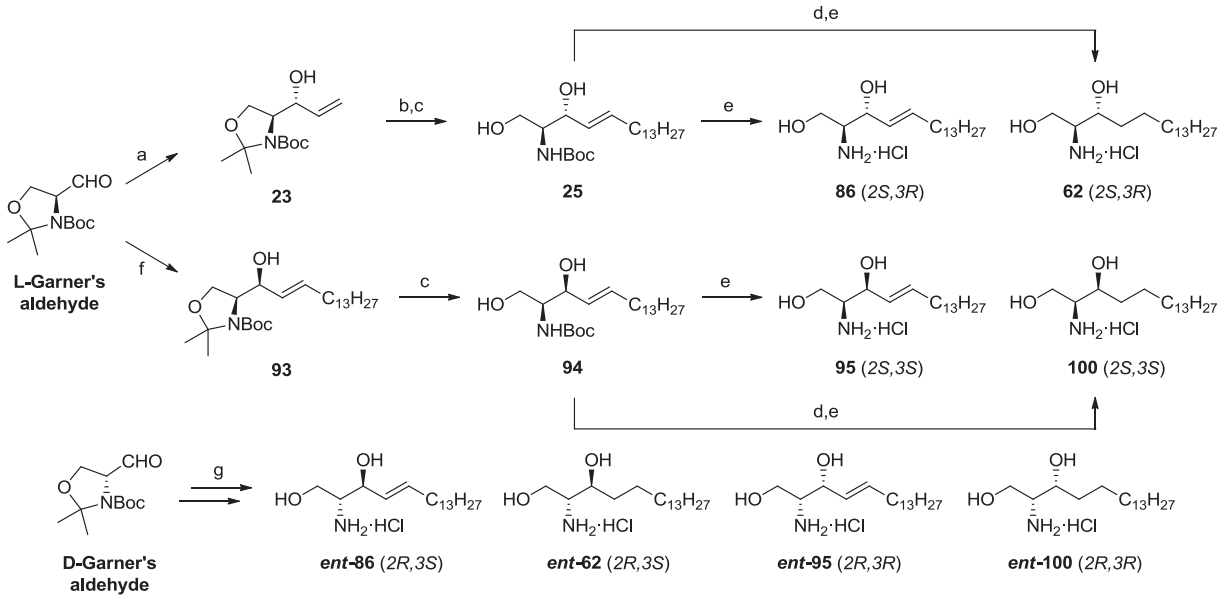

Scheme 3. Reagents and conditions: (a) vinylmagnesium bromide, THF, −78 °C, 64%, dr = 86:14; (b) 1-pentadecene, Grubbs catalyst 2nd gen., CH_2Cl_2, reflux, 78%, *E*/*Z* = 94:6; (c) *p*-TsOH, MeOH, rt, 94% for **25**, 92% for **94**; (d) H_2, 5 wt% Rh on Al_2O_3, MeOH, rt, 91–97%; (e) AcCl, MeOH, 0 °C to rt, 84%-quant. yield (f) (i) 1-pentadecyne, $Cp_2Zr(H)Cl$, CH_2Cl_2, 0 °C (ii) Et_2Zn, CH_2Cl_2, −40 to rt, 75%, dr = 93:7, only *E*; (g) same sequence as from L-Garner's aldehyde.

hand, the *syn*-adducts were efficiently obtained from addition of 1-pentadecenylethylzinc [37] to Garner's aldehyde. Again, the key intermediate **94** proved to be spectroscopically and configurationally in agreement with reported literature data [38]. Despite minor amounts of the inseparable *Z* isomers were detected in these initial steps, pure *E* isomers could be obtained after further purification steps along the synthetic route. In an analogous manner, the 2*R* series was obtained from D-Garner's aldehyde.

The differently configured sphingosines were submitted to diazotransfer reaction with imidazole-1-sulfonyl azide (ISA·HCl) [39], a process that courses with retention of configuration at the azide carbon [40,41] (Scheme 4). Gratifyingly, the resulting azides were in agreement with the expected configuration, as evidenced by comparison of their optical rotations with those reported in the literature for azido diols **87** [42], **96** [43], and **112** [44]. In addition, enantiomeric purity of these azido diols, together with that of the unreported azido diol **101** was confirmed by chiral HPLC with ee higher than 95% in all cases (see Supporting Material). Site-selective phosphorylation with dimethylchlorophosphate and methyl ester removal with Me_3SiBr [45] afforded the required azidophosphates in 15–25% overall yields from the starting Garner's aldehydes.

2.2. S1PL inhibition

The above compounds were tested against recombinant human

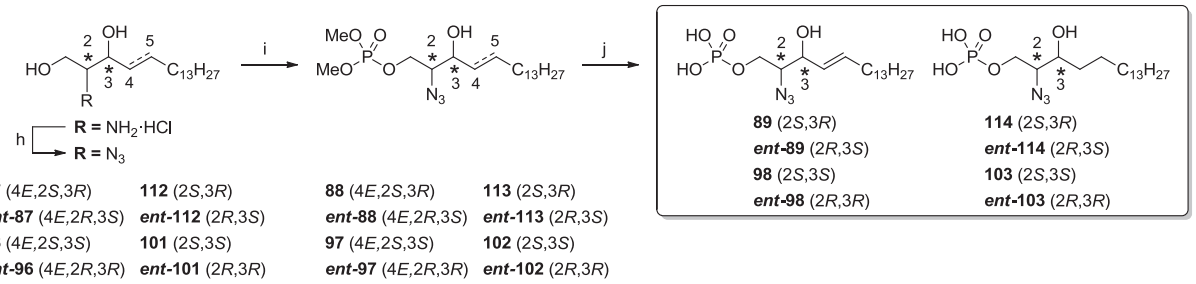

Scheme 4. Reagents and conditions: (a) 1*H*-imidazole-1-sulfonylazide hydrochloride, $CuSO_4 \cdot 5H_2O$, K_2CO_3, MeOH, rt, 80–91%; (b) Dimethyl chlorophosphate, *N*-methylimidazole, CH_2Cl_2, 0 °C to rt, 64–85%; (c) (i) Me_3SiBr, MeCN, 0 °C to rt (ii) MeOH/H_2O (95:5), rt, 56–71%.

(hS1PL) [26] and bacterial (*Symbiobacterium thermophilum*, StS1PL) [11] enzyme sources, using our previously developed fluorogenic substrate [46]. The results are collected in Table 1.

Compound **1**, designed as a mimic of the S1PL reaction intermediate **D** (see Scheme 1) behaved as a weak inhibitor (around 20% inhibition at 250 μM) in both hS1PL and StS1PL, while pyridoxine-5′-phosphate was practically devoid of activity. The presence of the sphingoid moiety in **12** and **32** led to more potent inhibitors, with IC_{50} values in the range of 50–80 μM for both enzymes.

Despite comparable IC_{50} values for **12** and **32** on each of the enzyme sources, a slight selectivity towards the bacterial enzyme was observed. Furthermore, the presence of a double bond at the C4–C5 position of the sphingoid backbone seemed not crucial for S1PL inhibition. A putative unspecific inhibition due to the triethylammonium counterion present in **12** and **32** was disregarded since incubation of both enzymes at different concentrations of triethylamine hydrochloride (500–0.5 μM range) did not affect the enzymatic activity (results not shown). The modest results obtained with enzyme intermediate mimics **1**, **12**, and **32**, initially designed to occupy the enzyme PLP binding site, could be explained by their inability to displace the cofactor from its Schiff base with the postulated Lys residue at the active site (Scheme 1). In addition, the bulkiness of **12** and **32** may prevent their access through the channel linking the active site with the cytosol, as observed in the X-ray structure reported for hS1PL [26].

Unlike the above compounds, all the azidophosphate analogs synthesized in this work behaved as low μM inhibitors on the two S1PL tested (Table 1). However, despite the subtle activity differences observed, some trends are worthy of mention. As StS1PL inhibitors, unsaturated derivatives **89**, ***ent*-89**, **98** and ***ent*-98**, showed IC_{50} values in the range of 10–16 μM, around 2-fold more active than their saturated analogs **114**, ***ent*-114**, **103** and ***ent*-103**, for which an IC_{50} value around 25 μM was determined in all cases. On the other hand, as hS1PL inhibitors, the *anti*-configured compounds **89**, ***ent*-89** and ***ent*-114** were the most active compounds of this series, with IC_{50} values of 10.1, 5.2 and 10.8 μM, respectively. Interestingly, the naturally configured (2*S*,3*R*) azidophosphate **114** (IC_{50} = 25.7 μM) was not as active as the above derivatives. The inhibition constants (K_i) against hS1PL showed a competitive inhibition pattern in all cases, with K_i values in the 5–40 μM range (See Supporting) and a good correlation with the corresponding IC_{50} values. However, despite the similar inhibitory trends, compounds ***ent*-89** and ***ent*-114**, both with the non-natural 2*R*, 3*S* configuration at the sphingoid backbone, were the most active stereoisomers of the series (Table 1 and Fig. 3). For the naturally configured series, **89** was found to be about two-fold more potent than its saturated analog **114**.

Finally, in order to study the contribution of the phosphate group on S1PL activity, the corresponding azidodiols (Scheme 4) were also evaluated as hS1PL inhibitors. All compounds were inactive at 250 μM, thus suggesting that the presence of the phosphate group, or a suitable surrogate, at C1 is critical to ensure a strong enzyme binding.

Computer docking simulations allowed proposing similar binding modes for the active azido phosphates in the active center of StS1PL and hS1PL. Fig. 4 shows the bound poses of compounds **89** and ***ent*-89** in the active center of both enzymes (PDB codes 3MAD and 4Q6R) [26,47]. In agreement with the above suggestion, these poses show that the phosphate group can establish multiple interactions with residues of a previously identified anion binding site [11,48], *i.e.* residues Y105, N126, H129 and K317 of StS1PL, and residues Y150, N171, H174 and K359 of hS1PL, thus confirming the prominent role of the phosphate moiety.

The long aliphatic chain is always placed along the narrow hydrophobic access channel that communicates the active site of the proteins with the surface, while the azido and hydroxyl groups of both compounds are placed close to two aromatic residues (H201/Y249 in StS1PL and H242/F290 in hS1PL), which are at short

Table 1
Inhibitory activity of the synthesized compounds.

Compound	IC_{50} (μM)		K_I (μM)[a]
	StS1PL	hS1PL	hS1PL
12	47.0	81.1	nd
32	53.4	89.0	nd
89	12.9	10.1	9.1
***ent*-89**	13.8	5.2	5.6
98	16.0	28.8	20.4
***ent*-98**	11.7	22.9	17.5
103	27.2	21.8	16.4
***ent*-103**	24.3	28.3	36.7
114	25.0	25.7	19.0
***ent*-114**	25.7	10.8	6.3

Shaded rows correspond to dihydro analogs.
nd: not determined.
[a] Competitive inhibitors.

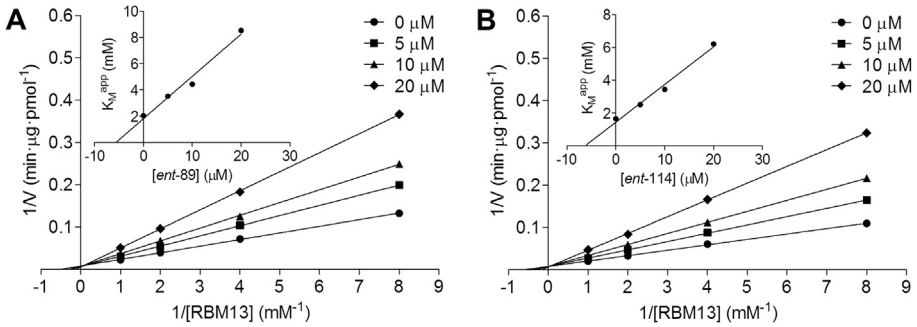

Fig. 3. Kinetics for the inhibition of hS1PL by *ent*-**89** (A) and *ent*-**114** (B). Double reciprocal plot of hS1PL incubated at different concentrations of substrate and compounds. Regression lines arise from data obtained in two different experiments performed in triplicate.

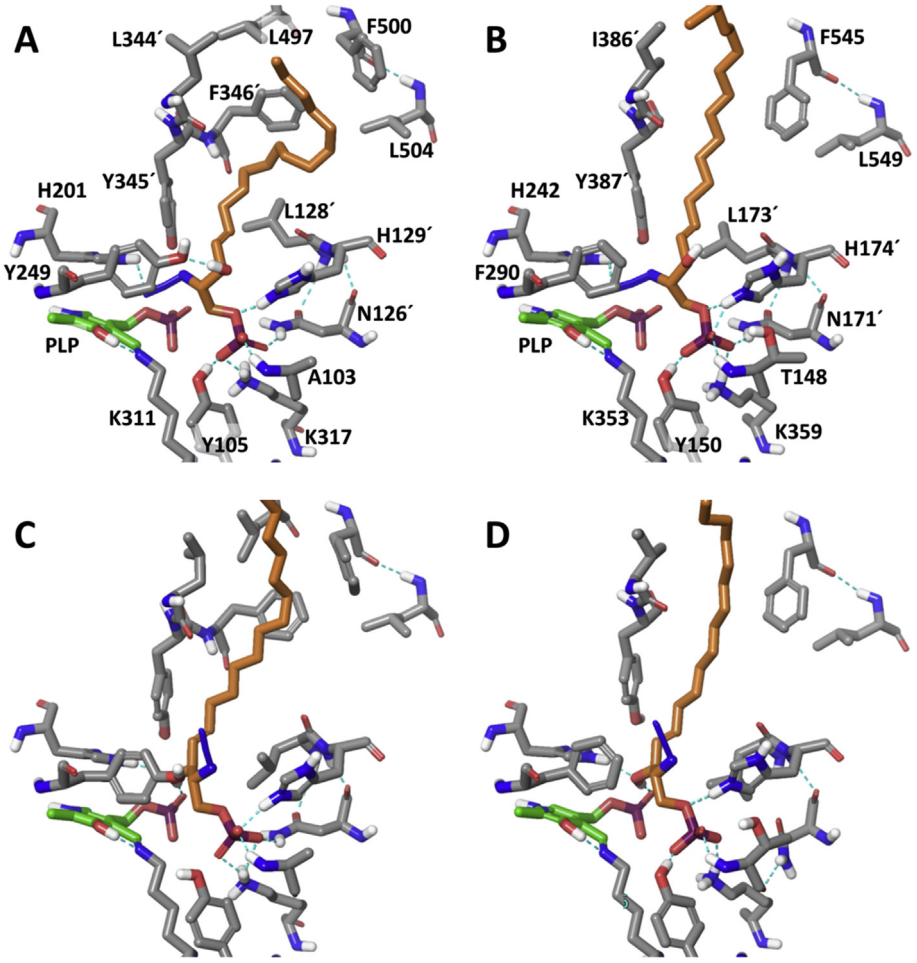

Fig. 4. Best docked poses of azido phosphates **89** (A, B) and ***ent*-89** (C, D) bound into the active site of StS1PL (A, C) and hS1PL (B, D), as determined by an Induced Fit Docking protocol. Azido phosphates and the PLP prosthetic group are highlighted in orange and green, respectively. Protein residues interacting with the inhibitors are shown and labelled, prime numbering indicates that residues belong to different subunits of the dimeric S1PL proteins. (For interpretation of the references to colour in this figure legend, the reader is referred to the web version of this article.)

distance of the PLP prosthetic group. The high similarity between the spatial arrangement of both compounds in the active sites of both proteins and the interactions that they stablish correlates well with their observed S1PL inhibitory activities. Furthermore, this docking analysis revealed that the presence or absence of the C4-double bond does not have a significant influence in the binding mode of the inhibitors, as illustrated by comparing the docked poses of azido phosphates **89** and ***ent*-89** (Fig. 4) with those of the corresponding saturated analogs **114** and ***ent*-114** (Fig. S14).

The similar behavior of the above azidophosphates as StS1PL and hS1PL inhibitors is also indicative of the similarities of both enzymes at their active site level. Hence, the more easily available StS1PL can be used as a reliable model of the human enzyme for putative inhibitors targeting the active site. This is not the case for inhibitors targeting the enzyme access channel, where the structural differences between both enzymes at that level may account

for the lack of activity on StS1PL observed for a recently reported potent hS1PL inhibitor [48]. These observations justify the development of an engineered StSPL as a model for the discovery of S1PL inhibitors [25].

3. Conclusion

In summary, two kinds of S1PL inhibitors have been designed and tested using bacterial (StS1PL) and human (hS1PL) enzyme sources. Amino phosphates **1**, **12**, and **32**, mimicking the intermediate aldimines of the catalytic process, were weak inhibitors on both enzyme sources, probably due to the steric constraints imposed by the PLP moiety. On the other hand, all the azido phosphates behaved as competitive inhibitors in the low μM range, being the *anti*-isomers with the non-natural enantiomeric configuration slightly more potent inhibitors on hS1PL.

4. Experimental section

4.1. General

Unless otherwise stated, reactions were carried out under argon atmosphere. Dry solvents were obtained by passing through an activated alumina column on a Solvent Purification System (SPS). Methanol was dried over CaH_2 and distilled prior to use. Commercially available reagents and solvents were used with no further purification. All reactions were monitored by TLC analysis using ALUGRAM® SIL G/UV_{254} precoated aluminum sheets (Machery-Nagel). UV light was used as the visualizing agent and a 5% (w/v) ethanolic solution of phosphomolybdic acid as the developing agent. Flash column chromatography was carried out with the indicated solvents using flash-grade silica gel (37–70 μm). Preparative reversed-phase purifications were performed on a Biotage® Isolera™ One equipment with the indicated solvents using a Biotage® SNAP cartridge (KP-C18-HS, 12 g) at a flow rate of 12 mL/min. Yields refer to chromatographically and spectroscopically pure compounds, unless otherwise stated.

NMR spectra were recorded at room temperature on a Varian Mercury 400 instrument. The chemical shifts (δ) are reported in ppm relative to the solvent signal, and coupling constants (J) are reported in Hertz (Hz). ^{31}P chemical shifts are relative to an 85% H_3PO_4 external reference (0 ppm). For ^{13}C NMR spectra recorded in D_2O, a 0.5% (w/v) solution of DSS (4,4-dimethyl-4-silapentane-1-sulfonic acid) in D_2O was used as external reference (0 ppm). The following abbreviations are used to define the multiplicities in ^1H NMR spectra: s = singlet, d = doublet, t = triplet, q = quartet, dd = doublet of doublets, ddd = doublet of doublet of doublets, m = multiplet, br = broad signal and app = apparent. High Resolution Mass Spectrometry analyses were carried out on an Acquity UPLC system coupled to a LCT Premier orthogonal accelerated time-of-flight mass spectrometer (Waters) using electrospray ionization (ESI) technique. Optical rotations were measured at room temperature on a Perkin Elmer 341 polarimeter.

HPLC analyses were carried out on an Alliance HPLC system consisting of a 2695 Separation Module (Waters) coupled to a 2996 PDA detector (Waters) and a light scattering ELS-1000 detector (Polymer Laboratories). Column A corresponds to a Phenomenex® Lux Amylose-2 (250 × 4.60 mm) and column B corresponds to a Chiralpak® IA (250 × 4.60 mm). Hexane/isopropanol mixtures at a flow rate of 1 mL/min were used as mobile phase and the monitoring wavelength was set at 220 nm. Injection volume was 5 μL. Retention times correspond to peaks observed using the PDA detector.

All biochemical reagents were commercially available and were used without further purification. RBM13 [46], Garner's aldehyde [49] and ISA·HCl [39] were synthesized in our laboratories following previously described methods.

Bacterial S1PL from *Symbiobacterium thermophilum* (StS1PL) was expressed and purified in our laboratory following a modified procedure (see Supplementary Material) of a previously reported protocol [11].

4.2. Chemistry

4.2.1. General procedure 1: reductive amination between PLP and selected amines

To an ice cooled solution of the selected amine (0.1 mmol) in dry CH_3OH (3 mL) was added KO*t*Bu (2 equiv) and the mixture was stirred at rt for 30 min (Solution A). Simultaneously, KO*t*-Bu (2 equiv/mol of PLP) was added to a solution of PLP (1.3 eq.) in CH_3OH (3 mL) at 0 °C and the mixture was stirred at rt for 30 min (Solution B). Solution A was then added dropwise to solution B at 0 °C and the mixture was refluxed in the dark for 3 h, cooled to 0 °C and treated with $NaBH_4$ (1.3 equiv). After stirring at rt for 1 h, the reaction mixture was acidified by dropwise addition of 6 M aq. HCl and the solvent was evaporated to dryness to give a residue, which was purified as indicated below.

*4.2.1.1. Phosphopyridoxylethanolamine phosphate (**1**) and pyridoxine-5′-phosphate.* Compound **1** (pale yellow solid, 110 mg, 79%) was obtained from solution A (*O*-phosphorylethanolamine (50 mg, 0.36 mmol), KO*t*-Bu (80 mg, 0.71 mmol)), solution B (PLP monohydrate (122 mg, 0.46 mmol), KO*t*-Bu (103 mg, 0.92 mmol) and $NaBH_4$ (17 mg, 0.46 mmol), according to general procedure 1. The crude material was dissolved in 10 mM aq. NH_4HCO_3 and applied to a DEAE-Sephadex A-25-120 ion exchange column (10 g) previously equilibrated with the same buffer. Elution with a linear gradient from 10 to 300 mM aq. NH_4HCO_3 yielded the title compound. Pyridoxine-5′-phosphate (22 mg, white solid) was also isolated.

For **1**: ^1H NMR (400 MHz, D_2O) δ 7.68 (s, 1H), 4.86 (d, J = 6.3 Hz, 2H), 4.45 (s, 2H), 4.10–4.01 (m, 2H), 3.38–3.30 (m, 2H), 2.48 (s, 3H). ^{13}C NMR (101 MHz, D_2O) δ 165.7, 147.4, 137.6 (d, $J_{C\text{-}P}$ = 7.9 Hz), 134.12, 126.1, 64.2 (d, $J_{C\text{-}P}$ = 4.3 Hz), 62.3 (d, $J_{C\text{-}P}$ = 4.4 Hz), 50.7 (d, $J_{C\text{-}P}$ = 6.9 Hz), 47.0, 17.6. ^{31}P NMR (162 MHz, D_2O) δ 2.93, 2.76. HRMS calcd. for $C_{10}H_{19}N_2O_9P_2$ ($[M+H]^+$): 373.0566, found: 373.0565.

Pyridoxine-5′-phosphate: ^1H NMR (400 MHz, D_2O) δ 7.78 (s, 1H), 4.96 (d, J = 6.4 Hz, 2H), 4.85 (s, 2H), 2.49 (s, 3H). ^{13}C NMR (101 MHz, D_2O) δ 172.7, 146.8, 141.9, 136.7 (d, $J_{C\text{-}P}$ = 8.2 Hz), 128.1, 64.3 (d, $J_{C\text{-}P}$ = 4.3 Hz), 58.8, 18.1. ^{31}P NMR (162 MHz, D_2O) δ 2.01. HRMS calcd. for $C_8H_{13}NO_6P$ ($[M+H]^+$): 250.0481, found: 250.0486.

*4.2.1.2. Phosphopyridoxylsphinganine-1-phosphate (**12**).* Compound **12** (pale yellow solid, 40 mg, 71%) was obtained from solution A (4,5-dihydrosphingosine-1-phosphate, 30 mg, 0.08 mmol), KO*t*-Bu (18 mg, 0.16 mmol), solution B (PLP monohydrate (27 mg, 0.10 mmol), KO*t*-Bu (23 mg, 0.21 mmol) and $NaBH_4$ (4 mg, 0.10 mmol), according to general procedure 1. The title compound was purified by preparative RP chromatography (from 5 to 100% CH_3CN in 100 mM TEAA, pH 7.0 buffer).

$[\alpha]_D^{20} = -4.5$ (*c* 1.0, CH_3OH). ^1H NMR (400 MHz, CD_3OD) δ 7.83 (s, 1H), 5.01–4.92 (m, 2H), 4.54 (d, J = 13.8 Hz, 1H), 4.43 (d, J = 13.8 Hz, 1H), 4.29–4.21 (m, 1H), 4.18–4.09 (m, 1H), 4.02–3.95 (m, 1H), 3.26 (dt, J = 7.6, 3.7 Hz, 1H), 3.19 (q, J = 7.3 Hz, 6H), 2.47 (s, 3H), 1.72–1.17 (m, 37H), 0.90 (t, J = 6.9 Hz, 3H). ^{13}C NMR (101 MHz, CD_3OD) δ 157.9, 147.5, 134.5, 134.0 (d, $J_{C\text{-}P}$ = 8.1 Hz), 130.9, 69.5, 64.0 (d, $J_{C\text{-}P}$ = 6.5 Hz), 63.7 (d, $J_{C\text{-}P}$ = 4.6 Hz), 62.0 (d, $J_{C\text{-}P}$ = 4.9 Hz), 47.6, 44.6, 34.4, 33.1, 30.8, 30.8, 30.8, 30.7, 30.5, 27.1, 23.7, 17.7, 14.5, 9.2. ^{31}P NMR (162 MHz, CD_3OD) δ 2.78, 1.92. HRMS calcd. for $C_{26}H_{51}N_2O_{10}P_2$ ($[M+H]^+$): 613.3019, found: 613.3024.

*4.2.1.3. Phosphopyridoxyl sphingosine-1-phosphate (**32**).* Compound **32** (pale yellow solid, 47 mg, 74%) was obtained from solution A (sphingosine-1-phosphate, 34 mg, 0.09 mmol), KO*t*-Bu (20 mg, 0.18 mmol)), solution B (PLP monohydrate (31 mg, 0.12 mmol)), KO*t*-Bu (26 mg, 0.23 mmol) and $NaBH_4$ (4 mg, 0.12 mmol), according to general procedure 1. The title compound was purified by preparative RP chromatography (from 5 to 100% CH_3CN in 100 mM TEAA pH 7.0 buffer).

$[\alpha]_D^{20} = -14.1$ (*c* 1.0, CH_3OH). ^1H NMR (400 MHz, CD_3OD) δ 7.82 (s, 1H), 5.93–5.82 (m, 1H), 5.54 (dd, J = 15.4, 6.6 Hz, 1H), 4.99–4.92 (m, 2H), 4.58 (d, J = 13.9 Hz, 1H), 4.46 (app t, J = 5.8 Hz, 1H), 4.41 (d, J = 13.9 Hz, 1H), 4.23 (ddd, J = 11.7, 6.6, 3.4 Hz, 1H), 4.16–4.07 (m, 1H), 3.26 (ddd, J = 8.2, 5.1, 3.5 Hz, 1H), 3.19 (q, J = 7.3 Hz, 6H), 2.46 (s, 3H), 2.11 (dd, J = 14.1, 7.1 Hz, 2H), 1.56–1.17 (m, 31H), 0.90 (t, J = 6.9 Hz, 3H). ^{13}C NMR (101 MHz, CD_3OD) δ 157.2, 147.6, 135.9, 135.7, 133.2 (d, $J_{C\text{-}P}$ = 8.7 Hz), 131.4, 129.7, 71.2, 63.8 (d, $J_{C\text{-}P}$ = 6.9 Hz), 63.7 (d, $J_{C\text{-}P}$ = 4.8 Hz), 62.5 (d, $J_{C\text{-}P}$ = 4.8 Hz), 47.5, 45.5, 33.5, 33.1, 30.8, 30.8, 30.8, 30.8, 30.7, 30.5, 30.2, 23.7, 17.7, 14.5, 9.2. ^{31}P NMR (162 MHz, CD_3OD) δ 2.64, 1.76. HRMS calcd. for $C_{26}H_{49}N_2O_{10}P_2$ ($[M+H]^+$): 611.2862, found: 611.2859.

4.2.2. General procedure 2: copper-catalyzed diazo-transfer reaction

To a stirred mixture of the corresponding amine hydrochloride (0.70 mmol), K_2CO_3 (2.70 equiv) and $CuSO_4 \cdot 5H_2O$ (0.01 equiv) in MeOH (7 mL) was added ISA·HCl (1.20 equiv) in one portion. After stirring at rt overnight, the mixture was concentrated, diluted with H_2O (5 mL), acidified with 1 M aqueous HCl and extracted with EtOAc (3 × 10 mL). The combined organic layers were washed with brine (2 × 10 mL), dried over anhydrous $MgSO_4$, filtered and evaporated *in vacuo*. Purification of the residue by flash chromatography (from 0 to 25% EtAcO in hexane) gave the required compound.

*4.2.2.1. (2S,3R,4E)-2-azidooctadec-4-ene-1,3-diol (**87**).* Compound **87** (white solid, 152 mg, 91%) was obtained from **86** (173 mg, 0.52 mmol), K_2CO_3 (192 mg, 1.39 mmol), $CuSO_4 \cdot 5H_2O$ (0.8 mg, catalytic) and ISA·HCl (130 mg, 0.62 mmol), according to general procedure 2.

$[\alpha]_D^{20} = -34.6$ (*c* 1.0, $CHCl_3$) [lit. [42] $[\alpha]_D^{25} = -33.2$ (*c* 2.0, $CHCl_3$)]. ^1H NMR (400 MHz, $CDCl_3$) δ 5.89–5.75 (m, 1H), 5.59–5.48 (m, 1H), 4.28–4.21 (m, 1H), 3.84–3.73 (m, 2H), 3.51 (dd, J = 10.4, 5.5 Hz, 1H), 2.12–1.99 (m, 4H), 1.46–1.18 (m, 22H), 0.88 (t, J = 6.8 Hz, 3H). ^{13}C NMR (101 MHz, $CDCl_3$) δ 136.1, 128.1, 73.9, 66.9, 62.7, 32.5, 32.1, 29.8, 29.8, 29.8, 29.8, 29.7, 29.6, 29.5, 29.3, 29.1, 22.8, 14.2. HRMS calcd. for $C_{18}H_{35}N_3O_2Na$ ($[M+Na]^+$): 348.2627, found: 348.2637. R_T (Column B, hexane/isopropanol (96.5:3.5)): 16.5 min *ca.* 99% *ee*.

*4.2.2.2. (2R,3S,4E)-2-azidooctadec-4-ene-1,3-diol (**ent-87**).* Compound ***ent*-87** was obtained from ***ent*-86** following the procedure described for the preparation of **87**. Spectroscopic data were identical to those indicated for **87**.

$[\alpha]_D^{20} = +32.4$ (*c* 1.0, $CHCl_3$) [lit. [50] $[\alpha]_D^{24} = +39.3$ (*c* 1.0, $CHCl_3$)]. R_T (Column B, hexane/isopropanol (96.5:3.5)): 15.4 min *ca.* 99% *ee*.

*4.2.2.3. (2S,3S,4E)-2-azidooctadec-4-ene-1,3-diol (**96**).* Compound **96** (white solid, 217 mg, 82%) was obtained from **95** (272 mg, 0.81 mmol), K_2CO_3 (302 mg, 2.19 mmol), $CuSO_4 \cdot 5H_2O$ (1.3 mg, catalytic) and ISA·HCl (204 mg, 0.97 mmol), according to general procedure 2.

$[\alpha]_D^{20} = +1.0$ (*c* 1.0, $CHCl_3$) [lit [43]. $[\alpha]_D^{26} = +0.9$ (*c* 1.0, $CHCl_3$)]. ^1H NMR (400 MHz, $CDCl_3$) δ 5.86–5.74 (m, 1H), 5.52 (dd, J = 15.4, 7.1 Hz, 1H), 4.21 (app t, J = 6.2 Hz, 1H), 3.82 (dd, J = 11.4, 3.8 Hz, 1H), 3.70 (dd, J = 11.4, 6.4 Hz, 1H), 3.52–3.42 (m, 1H), 2.12–1.95 (m, 4H), 1.48–1.10 (m, 22H), 0.88 (t, J = 6.7 Hz, 3H). ^{13}C NMR (101 MHz, $CDCl_3$) δ 135.8, 128.4, 73.7, 67.7, 63.1, 32.4, 32.1, 29.8, 29.8, 29.7, 29.6, 29.5, 29.3, 29.1, 22.8, 14.3. HRMS calcd. for $C_{18}H_{35}N_3O_2Na$ ($[M+Na]^+$): 348.2627, found: 348.2595. R_T (Column A, hexane/isopropanol (95:5)): 15.3 min *ca.* 97% *ee*.

*4.2.2.4. (2R,3R,4E)-2-azidooctadec-4-ene-1,3-diol (**ent-96**).* Compound ***ent*-96** was obtained from ***ent*-95** following the procedure described for the preparation of **96**. Spectroscopic data were identical to those indicated for **96**.

$[\alpha]_D^{20} = -1.5$ (*c* 1.0, $CHCl_3$), [lit. [51] $[\alpha]_D^{24} = -2.4$ (*c* 0.3, $CHCl_3$)]. R_T (Column A, hexane/isopropanol (95:5)): 13.1 min *ca.* >99% *ee*.

*4.2.2.5. (2S,3R)-2-azidooctadecane-1,3-diol (**112**).* Compound **112** (white solid, 201 mg, 86%) was obtained from **62** (240 mg, 0.71 mmol), K_2CO_3 (265 mg, 1.92 mmol), $CuSO_4 \cdot 5H_2O$ (1.1 mg, catalytic) and ISA·HCl (179 mg, 0.85 mmol), according to general procedure 2.

$[\alpha]_D^{20} = +7.9$ (*c* 1.0, $CHCl_3$) [lit. [44] $[\alpha]_D^{24} = +4.1$ (*c* 0.5, $CHCl_3$)]. ^1H NMR (400 MHz, $CDCl_3$) δ 3.94–3.85 (m, 2H), 3.81–3.74 (m, 1H), 3.43 (dd, J = 10.1, 5.1 Hz, 1H), 2.03 (br s, 2H), 1.66–1.17 (m, 28H), 0.88 (t, J = 6.8 Hz, 3H). ^{13}C NMR (101 MHz, $CDCl_3$) δ 72.8, 67.0, 62.7, 33.9, 32.1, 29.8, 29.8, 29.8, 29.7, 29.7, 29.6, 29.5, 25.7, 22.8, 14.3. HRMS calcd. for $C_{18}H_{37}N_3O_2Na$ ($[M+Na]^+$): 350.2783, found: 350.2780. R_T (Column A, hexane/isopropanol (95:5)): 9.7 min *ca.* 98% *ee*.

*4.2.2.6. (2R,3S)-2-azidooctadecane-1,3-diol (**ent-112**).* Compound ***ent*-112** was obtained from ***ent*-62** following the procedure described for the preparation of **112**. Spectroscopic data were identical to those indicated for **112**.

$[\alpha]_D^{20} = -10.6$ (*c* 1.0, $CHCl_3$). R_T (Column A, hexane/isopropanol (95:5)): 7.8 min *ca.* 98% *ee*.

*4.2.2.7. (2S,3S)-2-azidooctadecane-1,3-diol (**101**).* Compound **101** (white solid, 225 mg, 80%) was obtained from **100** (289 mg, 0.86 mmol), K_2CO_3 (319 mg, 2.31 mmol), $CuSO_4 \cdot 5H_2O$ (1.4 mg, catalytic) and ISA·HCl (215 mg, 1.03 mmol), according to general procedure 2.

$[\alpha]_D^{20} = +7.3$ (*c* 1.0, $CHCl_3$). ^1H NMR (400 MHz, $CDCl_3$) δ 3.97–3.82 (m, 2H), 3.79–3.70 (m, 1H), 3.44 (dt, J = 6.1, 4.2 Hz, 1H), 2.07–2.00 (m, 1H), 1.91–1.86 (m, 1H), 1.62–1.20 (m, 28H), 0.88 (t, J = 6.8 Hz, 3H). ^{13}C NMR (101 MHz, $CDCl_3$) δ 72.5, 67.0, 63.8, 34.6, 32.1, 29.8, 29.8, 29.8, 29.8, 29.8, 29.7, 29.7, 29.6, 29.5, 25.7, 22.8, 14.3. HRMS calcd. for $C_{18}H_{37}N_3O_2Na$ ($[M+Na]^+$): 350.2783, found: 350.2755. R_T (Column A, hexane/isopropanol 96.5:3.5): 19.3 min *ca.* 95% *ee*.

*4.2.2.8. (2R,3R)-2-azidooctadecane-1,3-diol (**ent-101**).* Compound ***ent*-101** was obtained from ***ent*-100** following the procedure described for the preparation of **101**. Spectroscopic data were identical to those indicated for **101**.

$[\alpha]_D^{20} = -8.3$ (*c* 1.0, $CHCl_3$). R_T (Column A, hexane/isopropanol (96.5:3.5)): 15.2 min *ca.* 99% *ee*.

4.2.3. General procedure 3: site-selective phosphorylation of 1,3-diols

A solution of the starting diol (0.50 mmol) in CH_2Cl_2 (15 mL) at 0 °C was treated successively with *N*-methylimidazole (1.50 equiv) and dimethyl chlorophosphate (1.20 equiv). The reaction mixture was stirred at rt for 1 h and cooled again to 0 °C. The reaction was then quenched by dropwise addition of saturated aqueous NH_4Cl and stirred for 5 min. The mixture was extracted with CH_2Cl_2 (3 × 15 mL) and the combined organic layers were washed with brine (2 × 20 mL), dried over anhydrous $MgSO_4$ and filtered. Evaporation of the solvent afforded a crude mixture, which was purified as indicated below.

*4.2.3.1. (2S,3R,4E)-2-azido-3-hydroxyoctadec-4-en-1-yl dimethyl phosphate (**88**).* Compound **88** (colorless oil, 171 mg, 85%) was obtained from alcohol **87** (152 mg, 0.47 mmol), *N*-methylimidazole (56 μL, 0.70 mmol) and dimethyl chlorophosphate (60 μL, 0.56 mmol), according to general procedure 3. The title compound was purified by flash chromatography on silica gel (from 0 to 100% Et_2O in hexane).

$[\alpha]_D^{20} = -7.4$ (*c* 1.0, $CHCl_3$). ^1H NMR (400 MHz, $CDCl_3$) δ 5.88–5.77 (m, 1H), 5.57–5.46 (m, 1H), 4.28–4.15 (m, 3H), 3.82 (d, $J = 3.7$ Hz, 3H), 3.80 (d, $J = 3.7$ Hz, 3H), 3.57 (dd, $J = 10.3$, 5.8 Hz, 1H), 2.11–2.02 (m, 2H), 1.45–1.19 (m, 22H), 0.88 (t, $J = 6.8$ Hz, 3H). ^{13}C NMR (101 MHz, $CDCl_3$) δ 136.2, 127.7, 71.8, 67.2 (d, $J_{C\text{-}P} = 5.4$ Hz), 65.6 (d, $J_{C\text{-}P} = 6.6$ Hz), 54.7 (d, $J_{C\text{-}P} = 6.1$ Hz), 54.7 (d, $J_{C\text{-}P} = 6.1$ Hz), 32.4, 32.0, 29.8, 29.8, 29.8, 29.7, 29.6, 29.5, 29.3, 29.0, 22.8, 14.2. ^{31}P NMR (162 MHz, $CDCl_3$) δ 2.07. HRMS calcd. for $C_{20}H_{40}N_3O_5PNa$ ($[M+Na]^+$): 456.2603, found: 456.2603.

*4.2.3.2. (2R,3S,4E)-2-azido-3-hydroxyoctadec-4-en-1-yl dimethyl phosphate (**ent-88**).* Compound ***ent*-88** was obtained from ***ent*-87** following the procedure described for the preparation of **88**. Spectroscopic data were identical to those indicated for **88**.

$[\alpha]_D^{20} = +6.8$ (*c* 1.0, $CHCl_3$).

*4.2.3.3. (2S,3S,4E)-2-azido-3-hydroxyoctadec-4-en-1-yl dimethyl phosphate (**97**).* Compound **97** (colorless oil, 99 mg, 68%) was obtained from alcohol **96** (110 mg, 0.34 mmol), *N*-methylimidazole (40 μL, 0.51 mmol) and dimethyl chlorophosphate (44 μL, 0.41 mmol), according to general procedure 3. The title compound was purified by flash chromatography on silica gel (from 0 to 100% Et_2O in hexane).

$[\alpha]_D^{20} = -1.6$ (*c* 1.0, $CHCl_3$). ^1H NMR (400 MHz, $CDCl_3$) δ 5.86–5.72 (m, 1H), 5.49 (dd, $J = 15.4$, 6.9 Hz, 1H), 4.29–4.20 (m, 1H), 4.18–4.12 (m, 1H), 4.12–4.02 (m, 1H), 3.80 (s, 3H), 3.77 (s, 3H), 3.63–3.55 (m, 1H), 2.10–1.99 (m, 2H), 1.47–1.12 (m, 22H), 0.86 (t, $J = 6.6$ Hz, 3H). ^{13}C NMR (101 MHz, $CDCl_3$) δ 135.8, 127.8, 72.1, 67.2 (d, $J_{C\text{-}P} = 5.4$ Hz), 66.0 (d, $J_{C\text{-}P} = 7.0$ Hz), 54.7 (d, $J_{C\text{-}P} = 5.9$ Hz), 32.4, 32.0, 29.8, 29.8, 29.7, 29.6, 29.5, 29.3, 29.0, 22.8, 14.2. ^{31}P NMR (162 MHz, $CDCl_3$) δ 1.38. HRMS calcd. for $C_{20}H_{40}N_3O_5PNa$ ($[M+Na]^+$): 456.2603, found: 456.2591.

*4.2.3.4. (2R,3R,4E)-2-azido-3-hydroxyoctadec-4-en-1-yl dimethyl phosphate (**ent-97**).* Compound ***ent*-97** was obtained from ***ent*-96** following the procedure described for the preparation of **97**. Spectroscopic data were identical to those reported for **97**.

$[\alpha]_D^{20} = +2.3$ (*c* 1.0, $CHCl_3$).

*4.2.3.5. (2S,3R)-2-azido-3-hydroxyoctadecyl dimethyl phosphate (**113**).* Compound **113** (colorless oil, 66 mg, 76%) was obtained from alcohol **112** (65 mg, 0.20 mmol), *N*-methylimidazole (24 μL, 0.30 mmol) and dimethyl chlorophosphate (26 μL, 0.24 mmol), according to general procedure 3. The title compound was purified by flash chromatography on silica gel (from 0 to 100% Et_2O in hexane).

$[\alpha]_D^{20} = +22.0$ (*c* 1.0, $CHCl_3$). ^1H NMR (400 MHz, $CDCl_3$) δ 4.43–4.26 (m, 2H), 3.83 (d, $J = 4.7$ Hz, 3H), 3.80 (d, $J = 4.7$ Hz, 3H), 3.74–3.67 (m, 1H), 3.43–3.36 (m, 1H), 1.67–1.20 (m, 28H), 0.88 (t, $J = 6.8$ Hz, 3H). ^{13}C NMR (101 MHz, $CDCl_3$) δ 70.0, 67.3 (d, $J_{C\text{-}P} = 5.4$ Hz), 65.8 (d, $J_{C\text{-}P} = 5.9$ Hz), 54.9 (d, $J_{C\text{-}P} = 6.1$ Hz), 54.8 (d, $J_{C\text{-}P} = 6.1$ Hz), 33.6, 32.1, 29.8, 29.8, 29.8, 29.7, 29.7, 29.7, 29.5, 25.6, 22.8, 14.3. ^{31}P NMR (162 MHz, $CDCl_3$) δ 2.44. HRMS calcd. for $C_{20}H_{42}N_3O_5PNa$ ($[M+Na]^+$): 458.2760, found: 458.2765.

*4.2.3.6. (2R,3S)-2-azido-3-hydroxyoctadecyl dimethyl phosphate (**ent-113**).* Compound ***ent*-113** was obtained from ***ent*-112** following the procedure described for the preparation of **113**. Spectroscopic data were identical to those indicated for **113**.

$[\alpha]_D^{20} = -22.6$ (*c* 1.0, $CHCl_3$).

*4.2.3.7. (2S,3S)-2-azido-3-hydroxyoctadecyl dimethyl phosphate (**102**).* Compound **102** (colorless oil, 66 mg, 64%) was obtained from alcohol **101** (78 mg, 0.24 mmol), *N*-methylimidazole (29 μL, 0.36 mmol) and dimethyl chlorophosphate (31 μL, 0.29 mmol), according to general procedure 3. The title compound was purified by flash chromatography on silica gel (from 0 to 1% CH_3OH in CH_2Cl_2).

$[\alpha]_D^{20} = +4.3$ (*c* 1.0, $CHCl_3$). ^1H NMR (400 MHz, $CDCl_3$) δ 4.35–4.27 (m, 1H), 4.25–4.16 (m, 1H), 3.82 (s, 3H), 3.80 (s, 3H), 3.71–3.64 (m, 1H), 3.57 (ddd, $J = 8.0$, 5.1, 3.3 Hz, 1H), 1.68–1.17 (m, 28H), 0.88 (t, $J = 6.8$ Hz, 3H). ^{13}C NMR (101 MHz, $CDCl_3$) δ 70.7, 67.6 (d, $J_{C\text{-}P} = 5.5$ Hz), 65.4 (d, $J_{C\text{-}P} = 6.8$ Hz), 54.8 (d, $J_{C\text{-}P} = 6.1$ Hz), 54.7 (d, $J_{C\text{-}P} = 6.1$ Hz), 34.3, 32.1, 29.8, 29.8, 29.8, 29.8, 29.7, 29.7, 29.6, 29.5, 25.8, 22.8, 14.2. ^{31}P NMR (162 MHz, $CDCl_3$) δ 1.96. HRMS calcd. for $C_{20}H_{42}N_3O_5PNa$ ($[M+Na]^+$): 458.2760, found: 458.2764.

*4.2.3.8. (2R,3R)-2-azido-3-hydroxyoctadecyl dimethyl phosphate (**ent-102**).* Compound ***ent*-102** was obtained from ***ent*-101** following the procedure described for the preparation of **102**. Spectroscopic data were identical to those indicated for **102**.

$[\alpha]_D^{20} = -3.4$ (*c* 1.0, $CHCl_3$).

4.2.4. General procedure 4: deprotection of phosphate esters with TMSBr

To an ice cooled solution of the starting dimethyl phosphate (0.20 mmol) in dry CH_3CN (8 mL), was added dropwise TMSBr (4.0 equiv). After stirring for 3 h at rt, the reaction mixture was concentrated under reduced pressure. The residue was then taken up in MeOH/H_2O (95:5, same reaction volume), stirred for an additional hour at rt and evaporated to dryness. The crude reaction mixture was dissolved in methanol and loaded on an Amberlite XAD-4 column (10 g), which had been washed thoroughly with acetone and then equilibrated with water. Elution with a linear gradient from 0 to 70% MeCN in H_2O provided the required compound.

*4.2.4.1. (2S,3R,4E)-2-azido-3-hydroxyoctadec-4-en-1-yl dihydrogen phosphate (**89**).* Compound **89** (pale yellow solid, 52 mg, 71%) was obtained from dimethyl phosphate **88** (78 mg, 0.18 mmol) and TMSBr (95 μL, 0.72 mmol), according to general procedure 4.

$[\alpha]_D^{20} = -18.5$ (*c* 1.0, CH_3OH). ^1H NMR (400 MHz, CD_3OD) δ 5.83–5.72 (m, 1H), 5.51 (dd, $J = 15.3$, 7.4 Hz, 1H), 4.16–4.08 (m, 2H), 3.98–3.89 (m, 1H), 3.64–3.56 (m, 1H), 2.13–2.02 (m, 2H), 1.48–1.21 (m, 22H), 0.90 (t, $J = 6.7$ Hz, 3H). ^{13}C NMR (101 MHz, CD_3OD) δ 136.0, 129.6, 73.1, 67.5 (d, $J_{C\text{-}P} = 7.8$ Hz), 67.1 (d, $J_{C\text{-}P} = 5.1$ Hz), 33.4, 33.1, 30.8, 30.8, 30.8, 30.8, 30.7, 30.6, 30.5, 30.2, 30.2, 23.7, 14.4. ^{31}P NMR (162 MHz, CD_3OD) δ 1.22. HRMS calcd. for $C_{18}H_{36}N_3O_5PNa$ ($[M+Na]^+$): 428.2290, found: 428.2287.

*4.2.4.2. (2R,3S,4E)-2-azido-3-hydroxyoctadec-4-en-1-yl dihydrogen phosphate (**ent-89**).* Compound ***ent*-89** was obtained from ***ent*-88** following the procedure described for the preparation of **89**. Spectroscopic data were identical to those indicated for **89**.

$[\alpha]_D^{20} = +16.8$ (*c* 1.0, CH_3OH).

*4.2.4.3. (2S,3S,4E)-2-azido-3-hydroxyoctadec-4-en-1-yl dihydrogen phosphate (**98**).* Compound **98** (pale yellow solid, 57 mg, 68%) was obtained from dimethyl phosphate **97** (90 mg, 0.21 mmol) and TMSBr (110 μL, 0.83 mmol), according to general procedure 4.

$[\alpha]_D^{20} = -5.1$ (*c* 0.7, $CHCl_3$). ^1H NMR (400 MHz, CD_3OD) 5.85–5.72 (m, 1H), 5.53 (dd, $J = 15.4$, 6.9 Hz, 1H), 4.20–4.04 (m, 2H), 3.96 (br s, 1H), 3.53 (br s, 1H), 2.14–2.01 (m, 2H), 1.62–1.19 (m, 22H), 0.90 (t,

J = 6.8 Hz, 3H). ^{13}C NMR (101 MHz, CD_3OD) δ 135.3, 130.1, 73.1, 67.7 (d, $J_{C\text{-}P}$ = 4.1 Hz), 66.9 (d, $J_{C\text{-}P}$ = 4.2 Hz), 33.4, 33.1, 30.8, 30.8, 30.7, 30.6, 30.5, 30.3, 30.2, 23.7, 14.4. ^{31}P NMR (162 MHz, CD_3OD) δ 3.05. HRMS calcd. for $C_{18}H_{36}N_3O_5PNa$ ($[M+Na]^+$): 428.2290, found: 428.2287.

*4.2.4.4. (2R,3R,4E)-2-azido-3-hydroxyoctadec-4-en-1-yl dihydrogen phosphate (**ent-98**).* Compound ***ent*-98** was obtained from ***ent*-97** following the procedure described for the preparation of **98**. Spectroscopic data were identical to those indicated for **98**.

$[\alpha]_D^{20}$ = +4.2 (*c* 0.7, $CHCl_3$).

*4.2.4.5. (2S,3R)-2-azido-3-hydroxyoctadecyl dihydrogen phosphate (**114**).* Compound **114** (pale yellow solid, 39 mg, 56%) was obtained from dimethyl phosphate **113** (75 mg, 0.17 mmol) and TMSBr (91 μL, 0.69 mmol), according to general procedure 4.

$[\alpha]_D^{20}$ = +21.3 (*c* 0.7, $CHCl_3$). ^{1}H NMR (400 MHz, CD_3OD) δ 4.31–4.21 (m, 1H), 4.09–3.98 (m, 1H), 3.61–3.49 (m, 2H), 1.64–1.21 (m, 28H), 0.90 (t, J = 6.7 Hz, 3H). ^{13}C NMR (101 MHz, CD_3OD) δ 71.6, 67.7 (d, $J_{C\text{-}P}$ = 6.6 Hz), 67.4 (d, $J_{C\text{-}P}$ = 3.1 Hz), 34.4, 33.1, 30.8, 30.8, 30.8, 30.7, 30.7, 30.7, 30.5, 26.6, 23.7, 14.5. ^{31}P NMR (162 MHz, CD_3OD) δ 1.58. HRMS calcd. for $C_{18}H_{38}N_3O_5PNa$ ($[M+Na]^+$): 430.2447, found: 430.2441.

*4.2.4.6. (2R,3S)-2-azido-3-hydroxyoctadecyl dihydrogen phosphate (**ent-114**).* Compound ***ent*-114** was obtained from ***ent*-113** following the procedure described for the preparation of **114**. Spectroscopic data were identical to those indicated for **114**.

$[\alpha]_D^{20}$ = −23.7 (*c* 0.7, $CHCl_3$).

*4.2.4.7. (2S,3S)-2-azido-3-hydroxyoctadecyl dihydrogen phosphate (**103**).* Compound **103** (pale yellow solid, 50 mg, 69%) was obtained from dimethyl phosphate **102** (78 mg, 0.18 mmol) and TMSBr (95 μL, 0.72 mmol), according to general procedure 4.

$[\alpha]_D^{20}$ = +8.4 (*c* 0.5, $CHCl_3$). ^{1}H NMR (400 MHz, CD_3OD) δ 4.19–4.05 (m, 2H), 3.73–3.65 (m, 1H), 3.57–3.50 (m, 1H), 1.63–1.18 (m, 28H), 0.90 (t, J = 6.8 Hz, 3H). ^{13}C NMR (101 MHz, CD_3OD) δ 71.7, 67.4 (d, $J_{C\text{-}P}$ = 5.1 Hz), 67.1 (d, $J_{C\text{-}P}$ = 7.6 Hz), 34.9, 33.1, 30.8, 30.8, 30.7, 30.7, 30.7, 30.5, 26.8, 23.7, 14.5. ^{31}P NMR (162 MHz, CD_3OD) δ 1.29. HRMS calcd. for $C_{18}H_{38}N_3O_5PNa$ ($[M+Na]^+$): 430.2447, found: 430.2445.

*4.2.4.8. (2R,3R)-2-azido-3-hydroxyoctadecyl dihydrogen phosphate (**ent-103**).* Compound ***ent*-103** was obtained from ***ent*-102** following the procedure described for the preparation of **103**. Spectroscopic data were identical to those indicated for **103**.

$[\alpha]_D^{20}$ = −8.1 (*c* 0.5, $CHCl_3$).

4.3. Fluorogenic assay of S1PL enzyme activity

Recombinant bacterial or human S1PL (50 μL from stock solutions in buffer A (StS1PL) or B (hS1PL), final concentration: 25 μg/mL for StS1PL and 3 μg/mL for hS1PL) was added to a mixture of **RBM13** (added from a stock solution in 0.5 M potassium phosphate buffer, pH 7.2; final concentration: 125 μM) and the putative inhibitors (added from stock solutions in water (for 1, 12, 32 and pyridoxine-5′-phosphate) or 1% (v/v) TRITON X-100 in water (for the series of azidophosphates)) in either buffer solution A (StS1PL) or B (hS1PL) (final volume: 100 μL). Buffer solution A corresponds to a 1 mM potassium phosphate buffer, pH 7.2, containing 100 mM NaCl, 1 mM EDTA, 1 mM DTT and 10 μM pyridoxal 5′-phosphate. Buffer solution B corresponds to a 100 mM HEPES buffer, pH 7.4, containing 0.1 mM EDTA, 0.05% Triton X-100, 0.01% Pluronic F127 (Biotium), and 100 μM pyridoxal 5′-phosphate. The mixture was incubated at 37 °C for 1 h and the enzymatic reaction was stopped by the addition of 50 μL of MeOH. Finally, 100 μL of a 200 mM glycine-NaOH buffer, pH 10.6, were added to the resulting solution and the mixture was incubated for 20 additional min at 37 °C in order to complete the β-elimination reaction. The amount of umbelliferone formed was determined on either a SpectraMax M5 (Molecular Devices) or Synergy 2 (BioTek) microplate readers ($\lambda_{ex/em}$ = 355/460 nm), using a calibration curve. IC_{50} values were determined by plotting percent activity versus log [I] and fitting the data to the log(inhibitor) *vs.* response equation in Prism 5 (GraphPad Software, La Jolla). Settings for curve adjustments were kept with their default values. The type of inhibition and the Ki values for active inhibitors were determined by Lineweaver-Burk or Dixon plots of assays performed with different concentrations of inhibitor and substrate.

4.4. Computational docking methods

All the computational work was carried out with the Schrödinger Suite 2015 [52], through its graphical interface Maestro [53]. Coordinates of StSPL and hSPL (PDB codes 3MAD and 4Q6R) [1,2] were obtained from the Protein Data Bank [54] at Brookhaven National Laboratory. The protein X-ray structures were prepared using the Protein Preparation Wizard [55–59] included in Maestro to remove solvent molecules, ions and bound ligands, adding hydrogens, setting protonation states [60] and minimizing the energies. The 3-hydroxypyridine and imino groups of the Lys-bound PLP prosthetic group were considered in their neutral state. The azido phosphate structures were built within Maestro and set up with the LigPrep module [61] to generate ionization states, as well as for geometry optimization previous to docking. Ligands were docked into the active site of S1PL using the Induced Fit Docking Protocol [62] of the Schrodinger Suite, which uses Glide XP [63–66] to perform the docking phase and takes into consideration the flexibility of the protein residues within a given distance (5 Å) from the bound ligands, in order to refine the geometries and scores of the docked poses.

Acknowledgments

We are grateful to Prof. Andreas Billich (Novartis) for a generous gift of recombinant hS1PL. Partial financial support from the “Ministerio de Ciencia e Innovación”, Spain (Project CTQ2014-54743-R is acknowledged). The authors also want to thank “Fundació la Marató de TV3” for financial support through Projects 20112130 and 20112132.

Appendix A. Supplementary data

Supplementary data related to this article can be found at http://dx.doi.org/10.1016/j.ejmech.2016.08.008.

References

[1] A. Kihara, S. Mitsutake, Y. Mizutani, Y. Igarashi, Metabolism and biological functions of two phosphorylated sphingolipids, sphingosine 1-phosphate and ceramide 1-phosphate, Prog. Lipid Res. 46 (2) (2007) 126–144.
[2] L. Lu, A.H. Barfejani, T. Qin, Q. Dong, C. Ayata, C. Waeber, Fingolimod exerts neuroprotective effects in a mouse model of intracerebral hemorrhage, Brain Res. 1555 (2014) 89–96.
[3] I.N. Singh, E.D. Hall, Multifaceted roles of sphingosine-1-phosphate: how does this bioactive sphingolipid fit with acute neurological injury? J. Neurosci. Res. 86 (2008) 1419–1433.
[4] L. Arana, P. Gangoiti, A. Ouro, M. Trueba, A. Gomez-Munoz, Ceramide and ceramide 1-phosphate in health and disease, Lipids Heal. Dis. 9 (1) (2010) 15.
[5] M. Maceyka, S. Spiegel, Sphingolipid metabolites in inflammatory disease, Nature 510 (7503) (2014) 58–67.
[6] S. Spiegel, S. Milstien, The outs and the ins of sphingosine-1-phosphate in immunity, Nat. Rev. Immunol. 11 (2011) 403–415.

[7] H. Rosen, R.C. Stevens, M. Hanson, E. Roberts, M.B.A.A. Oldstone, Sphingosine-1-Phosphate and its receptors: structure, signaling, and influence, Annu. Rev. Biochem. 82 (1) (2013) 637–662.
[8] T. Sanchez, T. Hla, Structural and functional characteristics of S1P receptors, J. Cell Biochem. 92 (5) (2004) 913–922.
[9] M. Adada, D. Canals, Y.A. Hannun, L.M. Obeid, Sphingosine-1-phosphate receptor 2: a review, Febs J. 280 (2013) 6354–6366.
[10] M.J. Pulkoski-Gross, J.C. Donaldson, L.M. Obeid, Sphingosine-1-phosphate metabolism: a structural perspective, Crit. Rev. Biochem. Mol. Biol. 50 (4) (2015) 298–313.
[11] F. Bourquin, H. Riezman, G. Capitani, M.G. Grutter, Structure and function of sphingosine-1-phosphate lyase, a key enzyme of sphingolipid metabolism, Structure 18 (8) (2010) 1054–1065.
[12] M. Ikeda, A. Kihara, Y. Kariya, Y.M. Lee, Y. Igarashi, Sphingolipid-to-glycerophospholipid conversion in SPL-null cells implies the existence of an alternative isozyme, Biochem. Biophys. Res. Commun. 329 (2) (2005) 474–479.
[13] W.L. Santos, K.R. Lynch, Drugging sphingosine kinases, ACS Chem. Biol. 10 (2015) 225–233.
[14] W. Stoffel, M. Grol, Chemistry and biochemistry of 1-desoxysphinganine-1-phosphonate (dihydrosphingosine-1-phosphonate), Chem. Phys. Lipids 13 (1974) 372–388.
[15] A. Boumendjel, S.P.F. Miller, Synthesis of an inhibitor of sphingosine- 1-phosphate lyase, Tetrahedron Lett. 35 (6) (1994) 819–822.
[16] P. Bandhuvula, Y.Y. Tam, B. Oskouian, J.D. Saba, The immune modulator FTY720 inhibits sphingosine-1-phosphate lyase activity, J. Biol. Chem. 280 (2005) 33697–33700.
[17] E.V. Berdyshev, J. Goya, I. Gorshkova, G.D. Prestwich, H.S. Byun, R. Bittman, V. Natarajan, Characterization of sphingosine-1-phosphate lyase activity by electrospray ionization-liquid chromatography/tandem mass Spectrometry quantitation of (2E)-hexadecenal, Anal. Biochem. (2011) 12–18.
[18] E. Loetscher, K. Schneider, C. Beerli, A. Billich, Assay to measure the secretion of sphingosine-1-phosphate from cells induced by S1P lyase inhibitors, Biochem. Biophys. Res. Commun. 433 (3) (2013) 345–348.
[19] A. Billich, C. Beerli, R. Bergmann, C. Bruns, E. Loetscher, Cellular assay for the characterization of sphingosine-1-phosphate lyase inhibitors, Anal. Biochem. 434 (2) (2013) 247–253.
[20] J.T. Bagdanoff, M.S. Donoviel, A. Nouraldeen, J. Tarver, Q. Fu, M. Carlsen, T.C. Jessop, H. Zhang, J. Hazelwood, H. Nguyen, S.D. Baugh, M. Gardyan, K.M. Terranova, J. Barbosa, J. Yan, M. Bednarz, S. Layek, L.F. Courtney, J. Taylor, A.M. Digeorge-Foushee, S. Gopinathan, D. Bruce, T. Smith, L. Moran, E. O'Neill, J. Kramer, Z. Lai, S.D. Kimball, Q. Liu, W. Sun, S. Yu, J. Swaffield, A. Wilson, A. Main, K.G. Carson, T. Oravecz, D.J. Augeri, Inhibition of sphingosine-1-phosphate lyase for the treatment of autoimmune disorders, J. Med. Chem. 52 (13) (2009) 3941–3953.
[21] J.T. Bagdanoff, M.S. Donoviel, A. Nouraldeen, M. Carlsen, T.C. Jessop, J. Tarver, S. Aleem, L. Dong, H. Zhang, L. Boteju, J. Hazelwood, J. Yan, M. Bednarz, S. Layek, I.B. Owusu, S. Gopinathan, L. Moran, Z. Lai, J. Kramer, S.D. Kimball, P. Yalamanchili, W.E. Heydorn, K.S. Frazier, B. Brooks, P. Brown, A. Wilson, W.K. Sonnenburg, A. Main, K.G. Carson, T. Oravecz, D.J. Augeri, Inhibition of sphingosine 1-phosphate lyase for the treatment of rheumatoid arthritis: discovery of (E)-1-(4-((1 R,2 S,3 R)-1,2,3,4-Tetrahydroxybutyl)-1 H -Imidazol-2-yl)ethanone oxime (LX2931) and (1 R,2 S,3 R)-1-(2-(Isoxazol-3-Yl)-1 H -imidazol-4-yl)butane-1,2,3,4-tetraol (LX2932), J. Med. Chem. 53 (2010) 8650–8662.
[22] S.R. Schwab, J.P. Pereira, M. Matloubian, Y. Xu, Y. Huang, J.G. Cyster, Lymphocyte sequestration through S1P lyase inhibition and disruption of S1P gradients, Science 309 (5741) (2005) 1735–1739.
[23] M. Ohtoyo, M. Tamura, N. Machinaga, F. Muro, R. Hashimoto, Sphingosine 1-phosphate lyase inhibition by 2-acetyl-4-(tetrahydroxybutyl)imidazole (THI) under conditions of vitamin B6 deficiency, Mol. Cell. Biochem. 400 (1–2) (2015) 125–133.
[24] M. Ohtoyo, N. Machinaga, R. Inoue, K. Hagihara, H. Yuita, M. Tamura, R. Hashimoto, J. Chiba, F. Muro, J. Watanabe, Y. Kobayashi, K. Abe, Y. Kita, M. Nagasaki, T. Shimozato, Component of caramel food coloring, THI, causes lymphopenia indirectly via a key metabolic intermediate, Cell Chem. Biol. 23 (5) (2016) 555–560.
[25] M.A. Argiriadi, D. Banach, E. Radziejewska, S. Marchie, J. DiMauro, J. Dinges, E. Dominguez, C. Hutchins, R.A. Judge, K. Queeney, G. Wallace, C.M. Harris, Creation of a S1P lyase bacterial surrogate for structure-based drug design, Bioorg. Med. Chem. Lett. (2016), http://dx.doi.org/10.1016/j.bmcl.2016.02.084.
[26] S. Weiler, N. Braendlin, C. Beerli, C. Bergsdorf, A. Schubart, H. Srinivas, B. Oberhauser, A. Billich, Orally active 7-substituted (4-benzyl-phthalazin-1-yl)-2-methyl-piperazin-1-yl]-nicotinonitriles as active-site inhibitors of sphingosine-1-phosphate lyase for the treatment of multiple sclerosis, J. Med. Chem. 57 (12) (2014) 5074–5084.
[27] J. Dinges, C.M. Harris, G.A. Wallace, M.A. Argiriadi, K.L. Queeney, D.C. Perron, E. Dominguez, T. Kebede, K.E. Desino, H. Patel, A. Vasudevan, Hit-to-lead evaluation of a novel class of sphingosine 1-phosphate lyase inhibitors, Bioorg. Med. Chem. Lett. 26 (9) (2016) 2297–2302.
[28] A. Delgado, M. Martínez-Cartró, Therapeutic potential of the modulation of sphingosine-1-phosphate receptors, Curr. Med. Chem. 23 (3) (2016) 242–264.
[29] M. Garrido, J.L. Abad, G. Fabrias, J. Casas, A. Delgado, Azide-tagged sphingolipids: new tools for metabolic flux analysis, ChemBioChem 16 (4) (2015) 641–650.
[30] R.J. Griffin, The medicinal chemistry of the azido group, Prog. Med. Chem. 31 (1994) 121–232.
[31] K. Tilley, M. Akhtar, D. Gani, The stereochemical course of decarboxylation, transamination and elimination reactions catalysed by *Escherichia Coli* glutamic acid decarboxylase, J. Chem. Soc. Perkin Trans. 1 (No. 21) (1994) 3079–3087.
[32] S.Y. Choi, J.E. Churchich, Glutamate decarboxylase side reactions catalyzed by the enzyme, Eur J Biochem. 160 (3) (1986) 515–520.
[33] I. Ojima, E.S. Vidal, Rhodium-catalyzed cyclohydrocarbonylation: application to the synthesis of (+)-Prosopinine and (−)-deoxoprosophylline †, J. Org. Chem. 63 (22) (1998) 7999–8003.
[34] K.P. Bhabak, D. Proksch, S. Redmer, C. Arenz, Novel fluorescent ceramide derivatives for probing ceramidase substrate specificity, Bioorg Med Chem 20 (20) (2012) 6154–6161.
[35] P. Wisse, H. Gold, M. Mirzaian, M.J. Ferraz, G. Lutteke, R.J.B.H.N. van den Berg, H. van den Elst, J. Lugtenburg, G.A. van der Marel, J.M.F.G. Aerts, J.D.C. Codée, H.S. Overkleeft, Synthesis of a panel of carbon-13-labelled (glyco)sphingolipids, European J. Org. Chem. 2015 (12) (2015) 2661–2677.
[36] T. Murakami, K. Furusawa, Efficient stereodivergent synthesis of erythro- and threo-sphingosines: unprecedented reversal of the stereochemistry in the addition, Tetrahedron 58 (45) (2002) 9257–9263.
[37] T. Murakami, K. Furusawa, Efficient stereodivergent synthesis of erythro- and threo-sphingosines: unprecedented reversal of the stereochemistry in the addition, Tetrahedron 58 (45) (2002) 9257–9263.
[38] P. Herold, Synthesis of D-erythro- and D-threo-sphingosine derivatives from l-serine, Helv. Chim. Acta 71 (2) (1988) 354–362.
[39] E.D. Goddard-Borger, R.V. Stick, An efficient, inexpensive, and shelf-stable diazotransfer reagent: imidazole-1-sulfonyl azide hydrochloride, Org Lett 9 (19) (2007) 3797–3800.
[40] P.T. Nyffeler, C.H. Liang, K.M. Koeller, C.H. Wong, The chemistry of amine-azide interconversion: catalytic diazotransfer and regioselective azide reduction, J. Am. Chem. Soc. 124 (36) (2002) 10773–10778.
[41] A.K. Pandiakumar, S.P. Sarma, A.G. Samuelson, Mechanistic studies on the diazo transfer reaction, Tetrahedron Lett. 55 (18) (2014) 2917–2920.
[42] M.S. Sandbhor, J.A. Key, I.S. Strelkov, C.W. Cairo, A modular synthesis of alkynyl-phosphocholine headgroups for labeling sphingomyelin and phosphatidylcholine, J. Org. Chem. 74 (22) (2009) 8669–8674.
[43] D. Enders, D.L. Whitehouse, J. Runsink, Diastereo- and enantioselective synthesis of L-threo- and D-erythvo-sphingosine, Chem. A Eur. J. 1 (6) (1995) 382–388.
[44] R.A. Fernandes, P. Kumar, A stereoselective synthesis of dihydrosphingosine, European J. Org. Chem. (2000) 3447–3449. No. 20.
[45] S. Grijalvo, A. Llebaria, A. Delgado, Straightforward access to simplified sphingosine-1-phosphate analogues, Synth. Commun. 37 (16) (2007) 2737–2751.
[46] C. Bedia, L. Camacho, J. Casas, J.L. Abad, A. Delgado, P.R. Van Veldhoven, G. Fabrias, Synthesis of a fluorogenic analogue of sphingosine-1-phosphate and its use to determine sphingosine-1-phosphate lyase activity, ChemBioChem 10 (5) (2009) 820–822.
[47] F. Bourquin, G. Capitani, M.G. Gruetter, PLP-dependent enzymes as entry and exit gates of sphingolipid metabolism, Protein Sci. 20 (2011) 1492–1508.
[48] P. Sanllehí, J.-L. Abad, J. Casas, J. Bujons, A. Delgado, Bacterial versus human sphingosine-1-phosphate lyase (S1PL) in the design of potential S1PL inhibitors, Bioorg. Med. Chem. (2016), http://dx.doi.org/10.1016/j.bmc.2016.07.033.
[49] A.D. Campbell, T.M. Raynham, C.W. Taylor, A simplified route to the (R)-Garner aldehyde and (S)-vinyl glycinol, Synthesis (Stuttg) (1998) 1707–1709.
[50] A.R. Parameswar, J.A. Hawkins, L.K. Mydock, M.S. Sands, A.V. Demchenko, Concise synthesis of the unnatural sphingosine and psychosine enantiomer, European J. Org. Chem. 2010 (17) (2010) 3269–3274.
[51] T.C. Nugent, T. Hudlicky, Chemoenzymatic synthesis of all four stereoisomers of sphingosine from chlorobenzene: glycosphingolipid precursors1a, J. Org. Chem. 63 (3) (1998) 510–520.
[52] Schrödinger Suite 2015 Update 2, Schrödinger, LLC, New York, NY, 2015.
[53] Maestro, Version 10.2, Schrödinger, LLC, New York, NY, 2015.
[54] H.M. Berman, J. Westbrook, Z. Feng, G. Gilliland, T.N. Bhat, H. Weissig, I.N. Shindyalov, P.E. Bourne, The protein data bank, Nucleic Acids Res 28 (1) (2000) 235–242.
[55] Schrödinger Protein Preparation Wizard 2015-2, Schrödinger, LLC, New York, NY, 2015.
[56] Schrödinger Epik, Version 2.4, Schrödinger, LLC, New York, NY, 2015.
[57] Schrödinger Impact, Version 5.9, Schrödinger, LLC, New York, NY, 2015.
[58] Schrödinger Prime, Version 3.2, Schrödinger, LLC, New York, NY, 2015.
[59] G.M. Sastry, M. Adzhigirey, T. Day, R. Annabhimoju, W. Sherman, Protein and ligand preparation: parameters, protocols, and influence on virtual screening enrichments, J. Comput. Aided Mol. Des. 27 (3) (2013) 221–234.
[60] M.H.M. Olsson, C.R. Søndergaard, M. Rostkowski, J.H. Jensen, PROPKA3: consistent treatment of internal and surface residues in empirical pKa predictions, J. Chem. Theory Comput. 7 (2) (2011) 525–537.
[61] LigPrep, Version 3.4, Schrödinger, LLC, New York, NY, 2015.
[62] Schrödinger Induced Fit Docking Protocol 2015-2, Scrödinger LCC, New York, NY, 2015.
[63] Schrödinger Glide, Version 6.7, Schrödinger, LLC, New York, NY, 2015.
[64] R.A. Friesner, J.L. Banks, R.B. Murphy, T.A. Halgren, J.J. Klicic, D.T. Mainz, M.P. Repasky, E.H. Knoll, M. Shelley, J.K. Perry, D.E. Shaw, P. Francis, P.S. Shenkin, Glide: a new approach for rapid, accurate docking and scoring. 1.

Method and assessment of docking accuracy, J Med Chem 47 (7) (2004) 1739–1749.
[65] T.A. Halgren, R.B. Murphy, R.A. Friesner, H.S. Beard, L.L. Frye, W.T. Pollard, J.L. Banks, Glide: a new approach for rapid, accurate docking and scoring. 2. Enrichment factors in database screening, J Med Chem 47 (7) (2004) 1750–1759.
[66] R.A. Friesner, R.B. Murphy, M.P. Repasky, L.L. Frye, J.R. Greenwood, T.A. Halgren, P.C. Sanschagrin, D.T. Mainz, Extra precision glide: docking and scoring incorporating a model of hydrophobic enclosure for protein-ligand complexes, J Med Chem 49 (21) (2006) 6177–6196.